Iterative Frequency-Domain Channel Estimation and Equalization for Single-Carrier Transmissions without Cyclic-Prefix

Hong Liu and Philip Schniter
The Dept. of Electrical and Computer Engineering
The Ohio State University, Columbus, OH 43210
Email: liu.523@osu.edu, schniter@ece.osu.edu

***Abstract*— Compared to the conventional time-domain methods, frequency-domain equalization (FDE) and frequency-domain channel estimation (FDCE) present computationally-efficient methods for the reception of single carrier (SC) transmissions. In this paper, we consider iterative FDE (IFDE) with explicit FDCE for non-cyclic-prefixed SC systems. First, an improved IFDE algorithm is presented based on soft iterative interference cancellation. Second, a new adaptive FDCE (AFDCE) algorithm based on per-tone Kalman filtering is proposed to track and predict the frequency-domain channel coefficients. The AFDCE algorithm employs across-tone noise reduction, exploits time-correlation between successive blocks, and adaptively updates the auto-regressive (AR) model coefficients, bypassing the need for priori knowledge of channel statistics. Finally, a block overlapping idea is proposed which facilitates the joint operation of IFDE and AFDCE. Simulation results show that, compared to other existing IFDE and adaptive channel estimation schemes, the proposed scheme offers lower mean-square-error (MSE) in channel prediction, lower bit error rate (BER) after decoding, and robustness to relatively fast fading channels.**

I. Introduction

Broadband wireless access systems offering high data rate transmission are likely to face severe multipath fading, with delay spread extends over tens or hundreds of symbol intervals. OFDM is a recognized multicarrier solution to combat multipath effects. However, it has the drawbacks of high peak-to-average power ratio (PAPR) and sensitivity to carrier-frequency offset. Single carrier (SC) transmission with frequency-domain equalization (FDE) is an alternative approach, which can deliver performance similar to OFDM, with essentially the same overall complexity [1]. Turbo equalization (TE) [2], [3] is a high-performance iterative reception scheme whereby the equalizer and decoder iteratively exchange soft information to jointly exploit channel structure and code structure. Combining TE with FDE can yield the performance gain with reduced computational cost compared to time- domain counterparts [4]–[6].

Efficient and effective channel estimation (CE) is crucial in system design. For OFDM transmission, various frequency-domain channel estimation (FDCE) schemes have been proposed to track and predict either slow-fading or fast-fading wireless channels with or without pilot symbols, with known or unknown channel statistic information [7]–[9]. For SC systems, time-domain channel estimation is the typical approach [10], [11], while FDCE is mostly based on known pilot symbols [12]–[14]. Furthermore, it has been observed that improved channel estimates may be obtained by incorporating soft information fed back from the decoder rather than hard symbol estimates [10], [11].

In this paper, we propose a new joint channel-estimation and equalization scheme for the reception of SC transmission over wireless channels with relatively fast fading and long delay spread. First, an improved iterative FDE (IFDE) algorithm is presented based on a frequency domain TE idea. Then, a new adaptive FDCE (AFDCE) algorithm based on soft-input Kalman filtering and frequency domain filtering is proposed to track and predict the channel on each frequency bin, which can exploit the time correlation between successive blocks and adaptively update the channel's AR model coefficients in the absence of any a priori statistical information. Finally, a block overlapping idea is adopted to implement joint IFDE and AFDCE. Our approach is different from other work on the subject in that:

1) IFDE in [4], [5] is first derived in the time domain and then approximated as FDE by exploiting the cyclic property of the equalizer. In contrast, our system model is set up in the frequency domain and IFDE is derived directly using reasonable approximations. Note, IFDE in [6] is a special case for vestigial side-band (VSB) modulation.
2) Some papers, such as [10], [11], assume a time-domain approach with soft inputs. Differently, we are interested in exploring FDCE with soft input to achieve lower computational complexity.
3) Other papers, such as [7], [9], [14], assume a frequency-domain Kalman filtering approach. However, all of them use pilot-symbol assisted CE. In contrast, we consider decision-directed CE, where the amplitudes of frequency-domain virtual symbols are random rather than constant as in [7], [9], [14] .

The rest of this paper is organized as follows. Section II briefly describes the communication system model. Section III introduces the minor modules of the proposed receiver, whereas the major IFDE and AFDCE modules are detailed in Section IV and Section V, respectively. Section VI discusses

implementation issues. Simulation results are presented in Section VII. Section VIII concludes the paper.

Throughout this paper, upper (lower) bold face letters will be used for matrices (column vectors). $\boldsymbol{A}^*$, $\boldsymbol{A}^T$, $\boldsymbol{A}^H$ and $\boldsymbol{A}^{-1}$ denote the conjugate, transpose, Hermitian transpose, and inverse of $\boldsymbol{A}$, respectively. We will use $\mathbf{I}$ for identity matrix, $\delta(p)$ for the Kronecker delta, $\|\cdot\|$ for l_2 norm, $\mathrm{R}e(\cdot)$ for the real part, $\mathcal{C}(\boldsymbol{a})$ denotes the circulant matrix with first column $\boldsymbol{a}$,$\mathcal{D}(\boldsymbol{a})$ for the diagonal matrix with $\boldsymbol{a}$ as its diagonal, $\mathrm{diag}(\cdot)$ for the extraction of the main diagonal of a matrix, $\boldsymbol{F}$ for the normalized fast Fourier transform (FFT) matrix where $F_{k,l} = \frac{1}{\sqrt{N}} e^{-j\frac{2\pi}{N}kl}$. $CN(\mu, \sigma^2)$ denotes the distribution of circular white Gaussian noise with mean μ and variance σ^2.

II. System Model

Consider coded single-carrier transmission where a bit stream $\{b_m\}$ is coded and mapped to uncorrelated finite alphabet symbols $\{s_n\}$ and transmitted over a noisy linear time-varying multipath wireless channel. The channel can be described by a length-N_h complex-valued impulse response $\{h_{n,l}\}_{l=0}^{N_h-1}$, where $h_{n,l}$ denotes the time-n response to an impulse applied at time $n-l$. The complex-valued observations $\{r_n\}$ are given by

$$r_n \;=\; \sum_{l=0}^{N_h-1} h_{n,l} s_{n-l} + u_n, \tag{1}$$

where $\{u_n\} \sim CN(0, \sigma_u^2)$.

For our joint IFDE and AFDCE scheme, we adopt block-wise processing with FFT block length N and effective output length N_d. For a very underspread channel (i.e., $f_d T_s \times N_h \ll 1$, where $f_d T_s$ denotes Doppler spread normalized by sampling frequency), it is common to assume that the channel is invariant within a block and varying across blocks. Therefore, we can define the block-based quantities $r_n(i) = r_{iN_d+n}$, $s_n(i) = s_{iN_d+n}$, $u_n(i) = u_{iN_d+n}$, and $h_l(i) = h_{iN_d+\frac{N}{2},l}$. Their vector counterparts are $\boldsymbol{r}(i) := [r_0(i), \ldots, r_{N-1}(i)]^T$, $\boldsymbol{s}(i) := [s_0(i), \ldots, s_{N-1}(i)]^T$, $\boldsymbol{u}(i) := [u_0(i), \ldots, u_{N-1}(i)]^T$, and $\boldsymbol{h}(i) := [h_0(i), \ldots, h_{N_h-1}(i), 0, \cdots, 0]^T$. Thus, the signal received during the i-th block can be expressed as

$$r_n(i) = \begin{cases} u_n^{(i)} + \sum_{l=0}^{n} h_l(i) s_{n-l}(i) \\ \quad + \sum_{l=n+1}^{N_h-1} h_l(i) s_{<n-l>_N}(i-1) & , \quad 0 \le n < N_h - 1, \\ u_n^{(i)} + \sum_{l=0}^{N_h-1} h_l(i) s_{n-l}(i), & N_h - 1 \le n < N, \end{cases} \tag{2}$$

where $<\; n \;>_N$ denotes n modulo N and $\{r_n(i)\}_{n=0}^{N_h-2}$ contains inter-block interference (IBI) from $\boldsymbol{s}(i-1)$.

III. Receiver Structure

Fig. 1 illustrates the block diagram for the reception of SC transmission without cyclic prefix (CP). The receiver will restore transmitted bits through following steps.

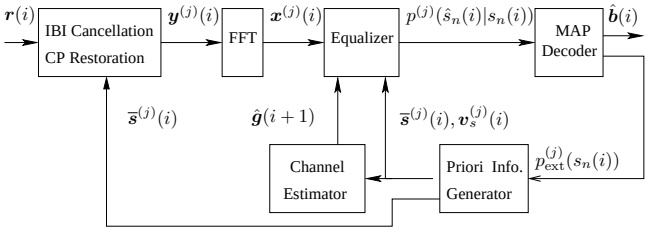

Fig. 1. Receiver structure.

1) Remove the IBI and restore the CP for the ith processing block $\boldsymbol{r}(i)$ as in [15], and transform it to the frequency-domain vector $\boldsymbol{x}^{(j)}(i)$ by taking the FFT.
2) Invert the channel in the frequency domain and generate symbol estimates $\hat{\boldsymbol{s}}(i)$. Extract the conditional probabilities $\left\{p^{(j)}\left(\hat{s}_n(i)|s_n(i)\right)\right\}_{n=0}^{N-1}$ from $\hat{\boldsymbol{s}}(i)$ by leveraging the constellation information of $\boldsymbol{s}(i)$.
3) Perform maximum a posteriori (MAP) decoding and calculate the extrinsic priori probability distribution $p_{\mathrm{ext}}^{(j)}(s_n(i))$. Output the hard bit estimate $\hat{\boldsymbol{b}}(i)$ at the last iteration.
4) Update the mean $\overline{\boldsymbol{s}}^{(j)}(i)$ and variance $\boldsymbol{v}_s^{(j)}(i)$ using $p_{\mathrm{ext}}^{(j)}(s_n(i))$ for the next round of equalization.
5) Feed $\overline{\boldsymbol{s}}^{(j)}(i)$ and $\boldsymbol{v}_s^{(j)}(i)$ into the channel estimator to smooth the current estimates and predict the channel for the next block.

Since steps 1-5 can be repeated several times for the same symbol block, we use superscript j to denote iteration index. The LOGMAP [16] algorithm is employed to perform MAP decoding. We now describe the IFDE (step 2) and AFDCE (step 5) in detail. More information about steps 1, 3 and 4 can be found in [3], [6], [15].

IV. Iterative Frequency Domain Equalization

For notational brevity, the iteration index j will be suppressed in the sequel. Assuming perfect IBI cancellation and CP restoration, the time-domain system model can be rewritten in matrix form as

$$\boldsymbol{y}(i) = \mathcal{C}\left(\boldsymbol{h}(i)\right)\boldsymbol{s}(i) + \boldsymbol{u}(i), \tag{3}$$

where $\boldsymbol{y}(i) := [y_0(i), \ldots, y_{N-1}(i)]$. Taking the discrete Fourier transform (DFT) on both sides of (3), we obtain

$$\boldsymbol{x}(i) = \boldsymbol{G}(i)\boldsymbol{t}(i) + \boldsymbol{w}(i), \tag{4}$$

where $\boldsymbol{x}(i)$,$\boldsymbol{t}(i)$ and $\boldsymbol{w}(i)$ denote DFTs of $\boldsymbol{y}(i)$,$\boldsymbol{s}(i)$ and $\boldsymbol{u}(i)$, respectively. Meanwhile, $\boldsymbol{g}(i)$=$\sqrt{N}\boldsymbol{F}\boldsymbol{h}(i)$, $\boldsymbol{G}(i) = \mathcal{D}\left(\boldsymbol{g}(i)\right)$, and $\boldsymbol{w}(i) \sim CN(\mathbf{0}, \sigma_w^2\mathbf{I})$. We refer to the elements in $\boldsymbol{t}(i)$ as *virtual subcarriers*.

Denoting the mean and variance of $\boldsymbol{s}(i)$ by $\overline{\boldsymbol{s}}(i)$ and $\boldsymbol{v}_s(i)$, respectively, it follows that

$$\overline{\boldsymbol{t}}(i) \;=\; \mathrm{E}[\boldsymbol{t}(i)] = \boldsymbol{F}\overline{\boldsymbol{s}}(i), \tag{5}$$

$$\begin{aligned} \boldsymbol{R}_{\boldsymbol{tt}}(i) &= \mathrm{E}\left[\left(\boldsymbol{t}(i) - \mathrm{E}[\boldsymbol{t}(i)]\right)\left(\boldsymbol{t}(i) - \mathrm{E}[\boldsymbol{t}(i)]\right)^H\right] \\ &= \boldsymbol{F}\,\mathcal{D}\left(\boldsymbol{v}_{\boldsymbol{s}}(i)\right)\boldsymbol{F}^H, \end{aligned} \tag{6}$$

$$\tilde{\boldsymbol{R}}_{\boldsymbol{tt}}(i) \;:=\; \mathcal{D}\left(\mathrm{diag}\left(\boldsymbol{F}\,\mathcal{D}\left(\boldsymbol{v}_{\boldsymbol{s}}(i)\right)\boldsymbol{F}^H\right)\right). \tag{7}$$

To simplify the equalization task, we choose to approximate (6) by (7). This is a practically reasonable approximation, and when all the elements of $\boldsymbol{s}(i)$ are independent and identically distributed (i.i.d), then $\tilde{\boldsymbol{R}}_{\boldsymbol{tt}}(i) = \boldsymbol{R}_{\boldsymbol{tt}}(i)$. Note that the approximate linear estimation (APPLE) algorithm proposed in [4], [5] is a special case of our approximation, where $\tilde{\boldsymbol{R}}_{\boldsymbol{tt}}(i) = \mathbf{I}$.

With $\bar{\boldsymbol{t}}(i)$ and $\tilde{\boldsymbol{R}}_{\boldsymbol{tt}}(i)$ as priors, the minimum mean square error (MMSE) estimate of $\boldsymbol{t}(i)$ is given by [17]

$$\hat{\boldsymbol{t}}(i) = \bar{\boldsymbol{t}}(i) + \tilde{\boldsymbol{R}}_{\boldsymbol{tt}}(i)\boldsymbol{G}^H(i)\boldsymbol{R}_{\boldsymbol{xx}}^{-1}\left(\boldsymbol{x}(i) - \boldsymbol{G}(i)\bar{\boldsymbol{t}}(i)\right), \quad (8)$$

$$\boldsymbol{R}_{\boldsymbol{xx}} = \boldsymbol{G}(i)\tilde{\boldsymbol{R}}_{\boldsymbol{tt}}(i)\boldsymbol{G}^H(i) + \sigma_w^2\mathbf{I}. \quad (9)$$

Denoting $\boldsymbol{v}_{\boldsymbol{t}}(i) = \operatorname{diag}\left(\tilde{\boldsymbol{R}}_{\boldsymbol{tt}}(i)\right)$, it can be shown that all the elements in $\boldsymbol{v}_{\boldsymbol{t}}(i)$ are identically equal to $v_t(i) = \frac{1}{N}\sum_{n=0}^{N-1} v_{s_n}(i)$, so that $\tilde{\boldsymbol{R}}_{\boldsymbol{tt}}(i) = v_t(i)\mathbf{I}$. Therefore the kth element of $\hat{\boldsymbol{t}}(i)$ can be written as

$$\hat{t}_k(i) = \bar{t}_k(i) + \underbrace{\frac{v_t(i)g_k^*(i)}{v_t(i)|g_k(i)|^2 + \sigma_w^2}}_{:=b_k(i)}\left(x_k(i) - g_k(i)\bar{t}_k(i)\right). \quad (10)$$

Next, we set $\hat{\boldsymbol{s}}(i) = \boldsymbol{F}^{-1}\hat{\boldsymbol{t}}(i)$. Assuming that the symbol estimation error has a Gaussian distribution,

$$p(\hat{s}_n(i)|s_n(i) = s) = \frac{1}{\sqrt{\pi\sigma_{n,i,s}^2}}\exp\left(-\frac{(\hat{s}_n(i) - u_{n,i,s})^2}{\sigma_{n,i,s}^2}\right), \quad (11)$$

$$u_{n,i,s} := \mathrm{E}\{\hat{s}_n(i)|s_n(i) = s\}, \quad (12)$$

$$\sigma_{n,i,s}^2 := \mathrm{var}\{\hat{s}_n(i)|s_n(i) = s\}, \quad (13)$$

where $s \in \mathcal{S}$ and where $\mathcal{S}$ denotes the symbol alphabet set. Furthermore, $u_{n,i,s}$ and $\sigma_{n,i,s}^2$ can be calculated as

$$u_{n,i,s} = \bar{s}_n(i) + \frac{s - \bar{s}_n(i)}{N}\sum_{k=0}^{N-1} b_k(i)g_k(i), \quad (14)$$

$$\sigma_{n,i,s}^2 = \frac{1}{N}\sum_{k=0}^{N-1}|b_k(i)|^2\left(|g_k(i)|^2\tilde{v}_n(i) + \sigma_w^2\right), \quad (15)$$

where $\tilde{v}_n(i) = \frac{1}{N}\sum_{k\neq n} v_{s_k}(i)$.

V. Adaptive Frequency Domain Channel Estimation

Conventional approaches to channel estimation rely on pilot symbols [12]–[14] or hard-decided symbols [8]. As shown in [10], [11], the soft output of a turbo equalizer can be exploited to improve CE performance. Therefore we propose a two-stage soft-input channel estimator which can take advantage of soft outputs from a IFDE and combat the error propagation effect. In the first stage, an M-order soft-input Kalman filter is adopted to estimate each frequency bin of the channel independently. Later, frequency-domain filtering is applied to refine the channel estimates. This two-stage approach can achieve a good tradeoff between performance and complexity. In addition, an adaptive filter similar to [9] is adopted to estimate the AR model coefficients for the Kalman filter. It can dynamically track the channel statistics and enable the AFDCE to achieve robust performance over a wide Doppler spread range.

A. Frequency Domain Soft Input Channel Estimation

In order to exploit the soft outputs of IFDE, we treat the transmitted symbol $s_k(i)$ as partially known and write it as:

$$s_k(i) = \bar{s}_k(i) + \tilde{s}_k(i), \quad (16)$$

where $\tilde{s}_k(i)$ is random variation around known $\bar{s}_k(i)$ with zero mean and variance $v_{s_k}(i)$. We assume that $\mathrm{E}[\tilde{s}_k(i)\tilde{s}_{k+p}(i+q)^*] = v_{s_k}(i)\delta_p\delta_q$. Notice that the virtual subcarrier vector $\boldsymbol{t}(i)$ is the DFT of $\boldsymbol{s}(i)$. Therefore,

$$t_k(i) = \bar{t}_k(i) + \tilde{t}_k(i), \quad (17)$$

where $\bar{t}_k(i)$ is given in (5) and $\tilde{t}_k(i)$ is a random variable with zero mean and variance $v_t(i)$. Consistent with approximation in (7), we assume $\mathrm{E}[\tilde{t}_k(i)\tilde{t}_{k+p}(i+q)^*] = v_t(i)\delta_p\delta_q$.

For a wide-sense stationary uncorrelated scattering (WSSUS) channel, and taking the above decomposition of $t_k(i)$ into consideration, we can formulate the state space model for the k-th frequency bin as

$$\underline{\boldsymbol{g}}_k(i) = \boldsymbol{A}\underline{\boldsymbol{g}}_k(i-1) + \underline{\boldsymbol{\eta}}_k(i), \quad (18)$$

$$x_k(i) = \boldsymbol{i}_1^H\underline{\boldsymbol{g}}_k(i)\bar{t}_k(i) + \boldsymbol{i}_1^H\underline{\boldsymbol{g}}_k(i)\tilde{t}_k(i) + w_k(i), \quad (19)$$

where $\underline{\boldsymbol{g}}_k(i) = [g_k(i), g_k(i-1), \cdots, g_k(i-M+1)]^T$, $\underline{\boldsymbol{\eta}}_k(i) = [\eta_k(i), 0, \cdots, 0]^T$, and $\eta_k(i) \sim \mathcal{CN}(0, \sigma_{\eta_k}^2)$. Also $\boldsymbol{i}_k$ denotes a length-M vector with 1 in the kth position and zeros elsewhere, and

$$\boldsymbol{A} = \begin{bmatrix} \alpha_1 & \alpha_2 & \cdots & \alpha_{M-1} & \alpha_M \\ 1 & 0 & \ddots & \ddots & 0 \\ 0 & 1 & \ddots & \ddots & 0 \\ \vdots & \ddots & \ddots & \ddots & \vdots \\ 0 & 0 & \cdots & 1 & 0 \end{bmatrix}, \quad (20)$$

where $\{\alpha_l\}_{l=1}^M$ are the AR model coefficients. Given the channel statistics, $\{\alpha_l\}_{l=1}^M$ and $\sigma_{\eta_k}^2$ can be obtained by applying the extended Yule-Walker method, and it can be shown that the AR coefficients are the same for all the k.

Let us denote $v_k(i) = g_k(i)\tilde{t}_k(i) + w_k(i)$ as the combinational noise term. Then we can show that $v_k(i)$ is also zero mean noise, as $w_k(i)$, but with different variance. In fact,

$$\bar{v}_k(i) = \mathrm{E}[v_k(i)] = \mathrm{E}[g_k(i)\tilde{t}_k(i) + w_k(i)] = 0, \quad (21)$$

$$\sigma_{v_k(i)}^2 = \mathrm{E}[v_k(i)v_{k+p}^*(i+q)] = \left(v_t(i)\sum_{l=0}^{N_h-1}\sigma_{h_l}^2 + \sigma_w^2\right)\delta_p\delta_q. \quad (22)$$

Here we made the assumption that $\mathrm{E}[h_l(i)h_{l+p}(i+q)] = \sigma_{h_l}^2\mathcal{J}_0(2\pi N f_d T_s q)\delta_p$, where $\mathcal{J}_0()$ is the zero-th order Bessel function. Therefore (18) and (19) can be rewritten as:

$$\underline{\boldsymbol{g}}_k(i) = \boldsymbol{A}\underline{\boldsymbol{g}}_k(i-1) + \underline{\boldsymbol{\eta}}_k(i), \quad (23)$$

$$x_k(i) = \boldsymbol{i}_1^H\underline{\boldsymbol{g}}_k(i)\bar{t}_k(i) + v_k(i). \quad (24)$$

It follows naturally that the Kalman filtering process can be

carried out iteratively through:

$$\hat{\underline{\boldsymbol{g}}}_k(i+1|\mathcal{X}_{k,i}) = \boldsymbol{A}\hat{\underline{\boldsymbol{g}}}_k(i|\mathcal{X}_{k,i}) \quad (25)$$

$$\hat{\underline{\boldsymbol{g}}}_k(i|\mathcal{X}_{k,i}) = \hat{\underline{\boldsymbol{g}}}_k(i|\mathcal{X}_{k,i-1}) + e_k(i)\boldsymbol{q}_{k,i} \quad (26)$$

$$e_k(i) = x_k(i) - \bar{t}_k(i)\boldsymbol{i}_1^H\hat{\underline{\boldsymbol{g}}}_k(i|\mathcal{X}_{k,i-1}) \quad (27)$$

$$\boldsymbol{q}_{k,i} = \boldsymbol{P}_{k,i|i-1}\bar{t}_k(i)^*\boldsymbol{i}_1\left(\bar{t}_k(i)\boldsymbol{i}_1^H\boldsymbol{P}_{k,i|i-1}\boldsymbol{i}_1\bar{t}_k^*(i) + \sigma^2_{v_k(i)}\right)^{-1} \quad (28)$$

$$\boldsymbol{P}_{k,i+1|i} = \boldsymbol{A}(\mathbf{I} - \boldsymbol{q}_{k,i}\bar{t}_k(i)\boldsymbol{i}_1^H)\boldsymbol{P}_{k,i|i-1}\boldsymbol{A}^T + \mathcal{D}(\boldsymbol{\sigma}^2_{\boldsymbol{\eta}_{k,i}}), \quad (29)$$

where $\boldsymbol{P}_{k,i+1|i} := \mathrm{E}\left[\varepsilon_k(i+1)\varepsilon_k(i+1)^H\right]$, $\varepsilon_k(i+1) := \underline{\boldsymbol{g}}_k(i+1) - \hat{\underline{\boldsymbol{g}}}_k(i+1|\mathcal{X}_{k,i})$, and $\boldsymbol{\sigma}^2_{\boldsymbol{\eta}_{k,i}} = [\sigma^2_{\eta_k(i)}, 0, \cdots, 0]^T$. $\mathcal{X}_{k,i}$ denotes the set of all observations up to the i-th block, namely, $\mathcal{X}_{k,i} = \{\boldsymbol{x}_k(j)\}_{j=0}^{i}$.

B. Frequency Domain Filtering

The proposed channel estimator works efficiently, since it decouples the whole CE task into tracking each frequency bin and makes full use of all past data through Kalman filtering. However, additional estimation error may persist due to ignorance of the fact that elements of $\boldsymbol{g}(i)$ are correlated. Therefore, we refine the channel estimates by leveraging the known correlation structure that results when $N_h < N$.

If $\hat{\boldsymbol{g}}(i|\mathcal{X}_i) := [\hat{g}_0(i|\mathcal{X}_{0,i}), \hat{g}_1(i|\mathcal{X}_{1,i}), \cdots, \hat{g}_{N-1}(i|\mathcal{X}_{N-1,i})]^T$, then we can estimate $\boldsymbol{g}(i)$ by constrained least-squares as follows,

$$\hat{\boldsymbol{g}}(i) := \min_{\hat{\boldsymbol{g}}(i)\in\mathrm{span}(\boldsymbol{F}_{N\times N_h})} \| \hat{\boldsymbol{g}}(i) - \hat{\boldsymbol{g}}(i|\mathcal{X}_i) \|^2 \quad (30)$$

$$= \boldsymbol{F}_{N\times N_h}\boldsymbol{F}^H_{N\times N_h}\hat{\boldsymbol{g}}(i|\mathcal{X}_i). \quad (31)$$

Overall, (31) is equivalent to a frequency-domain filtering operation, which first transforms the frequency domain channel estimates into the time domain, then sets the coefficients with index larger than $N_h - 1$ equal to zero, and finally transforms it back to the frequency domain. Denote $\hat{\underline{\boldsymbol{G}}}(i|\mathcal{X}_i) := [\hat{\underline{\boldsymbol{g}}}_0(i|\mathcal{X}_{0,i}), \hat{\underline{\boldsymbol{g}}}_1(i|\mathcal{X}_{1,i}), \cdots, \hat{\underline{\boldsymbol{g}}}_{N-1}(i|\mathcal{X}_{N-1,i})]^T$ and $\hat{\underline{\boldsymbol{G}}}(i) := [\hat{\underline{\boldsymbol{g}}}_0(i), \hat{\underline{\boldsymbol{g}}}_1(i), \cdots, \hat{\underline{\boldsymbol{g}}}_{N-1}(i)]^T$. Then channel estimates in (26) can be refined by

$$\hat{\underline{\boldsymbol{G}}}(i) = \boldsymbol{F}_{N\times N_h}\boldsymbol{F}^H_{N\times N_h}\hat{\underline{\boldsymbol{G}}}(i|\mathcal{X}_i). \quad (32)$$

C. Adaptive Tracking of AR Model Coefficients

When the Doppler spread of the channel is unknown or varying over time, we can estimate the AR model coefficients by tracking the channel statistics. As we can see from (18) and (20),

$$g_k(i) = \boldsymbol{\alpha}^H\underline{\boldsymbol{g}}_k(i-1) + \eta_k(i), \quad (33)$$

where $\boldsymbol{\alpha} = [\alpha_1, \alpha_2, \cdots, \alpha_M]^H$. Based on the Yule-Walker equations, for a stationary channel it is easy to show:

$$\begin{aligned} &\boldsymbol{\alpha}^H = \boldsymbol{R}_{cross,i}\boldsymbol{R}_i^{-1}, \qquad \sigma^2_\eta = \boldsymbol{R}_i(0,0) - \boldsymbol{\alpha}^H\boldsymbol{R}_i\boldsymbol{\alpha}, \\ &\boldsymbol{R}_i = \mathrm{E}\{\underline{\boldsymbol{g}}_k(i)\underline{\boldsymbol{g}}_k^H(i)\}, \ \boldsymbol{R}_{cross,i} = \mathrm{E}\{g_k(i+1)\underline{\boldsymbol{g}}_k^H(i)\}. \end{aligned} \quad (34)$$

Similar to [9], we compute (34) by recursively estimating $\boldsymbol{R}_{cross,i}$ and $\boldsymbol{R}_i$ using an exponential window with forgetting factor λ, as follows.

$$\hat{\boldsymbol{R}}_i = \lambda\hat{\boldsymbol{R}}_{i-1} + \frac{(1-\lambda)}{N}\sum_{k=0}^{N-1}\hat{\underline{\boldsymbol{g}}}_k(i-1)\hat{\underline{\boldsymbol{g}}}_k^H(i-1), \quad (35)$$

$$\hat{\boldsymbol{R}}_{cross,i} = \lambda\hat{\boldsymbol{R}}_{cross,i-1} + \frac{(1-\lambda)}{N}\sum_{k=0}^{N-1}\hat{g}_k(i)\hat{\underline{\boldsymbol{g}}}_k^H(i-1). \quad (36)$$

Finally the variance of the driving noise $\eta_k(i)$ is estimated through

$$\hat{\eta}_k(i) = \hat{g}_k(i) - \hat{\boldsymbol{\alpha}}^H\hat{\underline{\boldsymbol{g}}}_k(i-1), \quad (37)$$

$$\hat{\sigma}^2_{\eta_{k,i}} = \lambda\hat{\sigma}^2_{\eta_{k,i-1}} + (1-\lambda)\hat{\eta}_k(i)\hat{\eta}_k^*(i). \quad (38)$$

VI. Implementation Description

A. Block Overlapping

As mentioned in [6], due to causal channel dispersion and lack of CP, the symbols near the end of the block contribute little energy to the observation. As a result, these symbols are prone to estimation errors. Though the CP restoration procedure attempts to mitigate this problem, the procedure itself makes use of end-of-block symbol estimates which fail to converge to reliable values. In addition, the symbol estimates near the beginning of the block are contaminated by both IBI cancellation and CP restoration, due to imperfect CE and symbol estimation. Therefore the block overlapping technique shown in Fig. 2 is employed to avoid those unreliable tentative symbol estimates. For each block, only N_d (out of N) symbol estimates (show in grey) are retained as final estimates. As a result, the channel estimator must also work on overlapped blocks accordingly. More precisely, the channel equalizer and estimator are combined in the following manner: First, $\hat{\boldsymbol{s}}_d(i-1)$ in $\hat{\boldsymbol{s}}(i-1)$ is detected and output to the queue. Meanwhile, part of it is fed back to block $\hat{\boldsymbol{s}}(i-2)$ in order to update channel estimate $\hat{\underline{\boldsymbol{g}}}(i-2)$ and then predict $\hat{\boldsymbol{g}}(i)$. Then $\hat{\boldsymbol{s}}(i)$ is estimated based on $\hat{\boldsymbol{g}}(i)$ and $\hat{\boldsymbol{s}}_d(i)$ is output to the queue. Similarly, part of $\hat{\boldsymbol{s}}_d(i)$ is fed back to block $\hat{\boldsymbol{s}}(i-1)$ to update channel estimate $\hat{\underline{\boldsymbol{g}}}(i-1)$ and then predict $\hat{\boldsymbol{g}}(i+1)$. Through this interactive process, the receiver can achieve the superior BER and MSE performance as shown in Section VII.

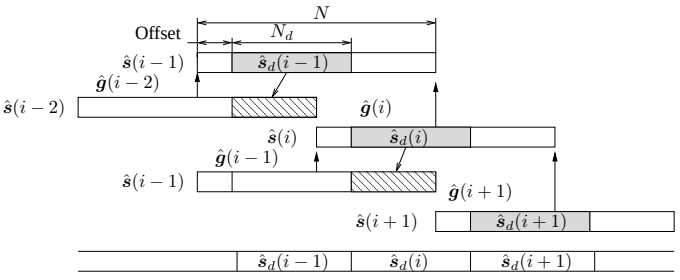

Fig. 2. The frame-overlapping scheme.

B. Algorithm Summary

Table I summarizes the major steps involved in joint IFDE and AFDCE. For notational brevity, the block index i is suppressed in the sequel except with $\hat{\underline{\boldsymbol{g}}}_k$, $\hat{\underline{\boldsymbol{G}}}$ and $\boldsymbol{P}_k$. The DFT operator stands for the Discrete Fourier Transform.

TABLE I
JOINT IFDE AND AFDCE ALGORITHM

Iterative Frequency Domain Equalization
Input: $[y_0 \cdots y_{N-1}]^T$, $[p(s_0) \cdots p(s_{N-1})]^T$, σ_w^2
Initialization: $[x_0 \cdots x_{N-1}]^T \leftarrow \text{DFT}[y_0 \cdots y_{N-1}]^T$ $[g_0 \cdots g_{N-1}]^T \leftarrow \text{DFT}[\hat{h}_0 \cdots \hat{h}_{N_h-1}\, \mathbf{0}_{1\times(N-N_h)}]^T$
Pre-equalization: compute $[\overline{s}_0 \cdots \overline{s}_{N-1}]^T$ and $[v_{s_0} \cdots v_{s_{N-1}}]^T$ $v_t = \frac{1}{N}\sum_{n=0}^{N-1} v_{s_n}$
Equalization: $[\overline{t}_0 \cdots \overline{t}_{N-1}]^T \leftarrow \text{DFT}[\overline{s}_0 \cdots \overline{s}_{N-1}]^T$ $\hat{t}_k = \overline{t}_k + \frac{v_t g_k^*}{v_t\lvert g_k\rvert^2+\sigma_w^2}(x_k - g_k\overline{t}_k) \quad \forall k$ $[\hat{s}_0 \cdots \hat{s}_{N-1}]^T \leftarrow \text{DFT}^{-1}[\hat{t}_0 \cdots \hat{t}_{N-1}]^T$
Post-equalization: compute $[p(\hat{s}_0\lvert s_0=s) \cdots p(\hat{s}_{N-1}\lvert s_{N-1}=s)]^T$
Adaptive Frequency Domain Channel Estimation
Channel estimate update and refinement: $\sigma_{v_k}^2 = v_t\sum_{l=0}^{N_h-1}\sigma_{h_l}^2 + \sigma_w^2$ $\boldsymbol{q}_k = \boldsymbol{P}_{k,i-1}\overline{t}_k\boldsymbol{i}_1(\overline{t}_k\boldsymbol{i}_1^H\boldsymbol{P}_{k,i-1}\boldsymbol{i}_1\overline{t}_k^* + \sigma_{v_k}^2)^{-1}$ $e_k = x_k - \overline{t}_k\boldsymbol{i}_1^H\underline{\hat{\boldsymbol{g}}}_{k,i}$ $\underline{\hat{\boldsymbol{g}}}_{k,i} = \underline{\hat{\boldsymbol{g}}}_{k,i} + e_k\boldsymbol{q}_k, \quad \underline{\hat{\boldsymbol{G}}}_i := [\underline{\hat{\boldsymbol{g}}}_{0,i}, \underline{\hat{\boldsymbol{g}}}_{1,i}, \cdots, \underline{\hat{\boldsymbol{g}}}_{N-1,i}]^T$ $\underline{\hat{\boldsymbol{G}}}_i = \boldsymbol{F}_{N\times N_h}\boldsymbol{F}_{N\times N_h}^H\underline{\hat{\boldsymbol{G}}}_i, \quad \underline{\hat{\boldsymbol{g}}}_{k,i+1} = \hat{\boldsymbol{A}}\underline{\hat{\boldsymbol{g}}}_{k,i}$ $\boldsymbol{P}_{k,i} = \hat{\boldsymbol{A}}(\mathbf{I} - \boldsymbol{q}_k\overline{t}_k\boldsymbol{i}_1^H)\boldsymbol{P}_{k,i-1}\hat{\boldsymbol{A}}^T + \mathcal{D}(\hat{\boldsymbol{\sigma}}_{\boldsymbol{\eta}_k}^2)$
AR model coefficient update: $\hat{\boldsymbol{R}} = \lambda\hat{\boldsymbol{R}} + \frac{(1-\lambda)}{N}\text{Re}\left(\sum_{k=0}^{N-1}\underline{\hat{\boldsymbol{g}}}_{k,i-1}\underline{\hat{\boldsymbol{g}}}_{k,i-1}^H\right)$ $\hat{\boldsymbol{R}}_{cross} = \lambda\hat{\boldsymbol{R}}_{cross} + \frac{(1-\lambda)}{N}\text{Re}\left(\sum_{k=0}^{N-1}\hat{g}_{k,i}\underline{\hat{\boldsymbol{g}}}_{k,i-1}^H\right)$ $\boldsymbol{\alpha}^H = \hat{\boldsymbol{R}}_{cross}\hat{\boldsymbol{R}}^{-1}$ $\hat{\eta}_k = \hat{g}_{k,i+1} - \hat{\boldsymbol{\alpha}}^H\underline{\hat{\boldsymbol{g}}}_{k,i} \quad \hat{\sigma}_{\eta_k}^2 = \lambda\hat{\sigma}_{\eta_k}^2 + (1-\lambda)\hat{\eta}_k\hat{\eta}_k^*$

VII. SIMULATION RESULT

In this section, we assess the performance of a receiver employing the proposed joint IFDE and AFDCE scheme.

A. System Parameter

We consider a SC non-CP system, where an information sequence is encoded with code generator $G(D) = (1 + D^2, 1 + D + D^2)$ and mapped to quaternary PSK (QPSK) symbols through Gray mapping. The time-varying channel is simulated using Jakes' model with delay spread $N_h = 128$ and constant power profile $\{\sigma_l^2 = \frac{1}{N_h}, l = 0, 1, \cdots, N_h - 1\}$. Our normalized Doppler spread is $f_dT_s \in \{0.00001, 0.00005\}$, which corresponds to a single-sided Doppler frequency spread $f_D \in \{100, 500\}$Hz with sampling rate $T_s^{-1} = 10$MHz. At the receiver side, the system parameters are set as: $N = 512$, Offset$= 50$, $N_d = 256$, $M = 2$, maximum iteration number $N_{iter} = 5$. The first transmitted block is known as the pilot block and used to initialize the channel estimator. All the simulation results were obtained by averaging over 100 independent experiments of 51200 consecutive symbols.

B. Performance Assessment

First, we compare the proposed IFDE plus AFDCE with the LMS_SCE algorithm suggested by Morelli, Sanguinetti and Mengali in [18]. Three different versions of AFDCE are tested: in ASKCE, we use adaptive soft-input Kalman-filter-based CE (KCE), where the inputs to the Kalman filter are the mean and variance of the virtual subcarrier symbols $\boldsymbol{t}$; in AHKCE, we use adaptive hard-input KCE, where the inputs to the Kalman filter are hard-decided virtual subcarrier symbols $\hat{\boldsymbol{t}}$ and the variance is set to $\mathbf{0}$; in ASHKCE, we use a hybrid of ASKCE and AHKCE which alternates between soft-input and hard-input mode depending on the approximate estimation error variance v_t. When v_t is above a threshold (set to 0.1 in our simulations), the algorithm works in AHKCE mode, while otherwise it works in the ASKCE mode. For LMS_SCE, we use stepsize $\mu = 0.1$ when $f_dT_s = 0.00001$ and $\mu = 0.5$ when $f_dT_s = 0.00005$. Our choice of μ is based on empirical observations, since no optimal choice of μ was specified in [18]. We compare the steady-state BER and MSE performances in Fig. 3 and Fig. 4, respectively. It can be seen that AHKCE and ASHKCE achieve better performance than LMS_SCE at all SNRs, where the performance difference increases as f_dT_s increases. This means that our proposed AFDCE scheme is more capable at tracking fast-fading channels than LMS_SCE. In addition, both AHKCE and ASHKCE perform within 1dB of the case that the channel is perfectly known. Though ASKCE does not perform well in the low-SNR regime, it performs slightly better than AHKCE in the high-SNR regime. ASHKCE combines the good features of both ASKCE and AHKCE, and thereby achieves the best performance among the algorithms.

In Fig. 5, we compare the dynamic tracking performance of ASKCE with an adaptive step-size version of LMS_SCE, using a channel in which $f_dT_s = 0.00001$ for the first 51200 symbols and $f_dT_s = 0.00005$ for the last 51200 symbols. During the intermediate phase (i.e., the middle 51200 symbols), the channel smoothly transitioned between the two Doppler frequencies. Fig. 5 shows that ASKCE achieves lower MSE than (adaptive-stepsize) LMS_SCE and that ASKCE demonstrates the ability to adapt to dynamic channel conditions while maintaining robust BER performance.

Finally, we compare the channel equalization performance of our proposed IFDE algorithm with Tuchler and Hagenauer's APPLE/MF algorithm from [4], [5]. Fig. 6 shows that our proposed IFDE plus ASHKCE scheme outperforms APPLE/MF plus either AHKCE or ASKCE.

VIII. CONCLUSION

In this paper, a joint FDE and CE receiver design for the reception of SC non-CP transmission was proposed. In particular, we detailed an improved IFDE algorithm based on frequency-domain turbo equalization, and proposed a novel AFDCE with robustness to fast fading. Simulation results show that the proposed IFDE-plus-AFDCE scheme demonstrates good performances in both stationary and non-stationary channels while maintaining low complexity as a consequence of

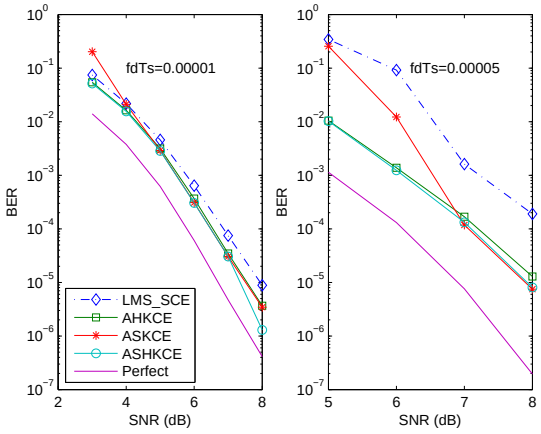

Fig. 3. BER versus SNR at steady state.

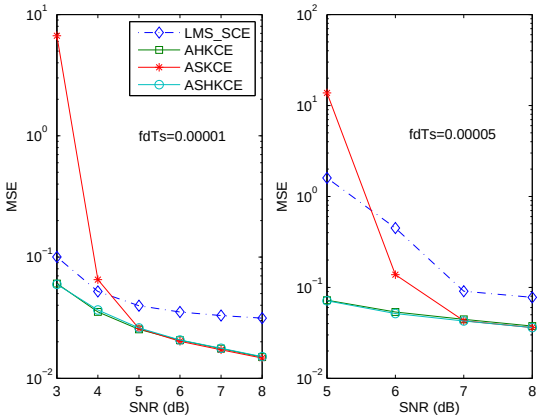

Fig. 4. MSE versus SNR at steady state.

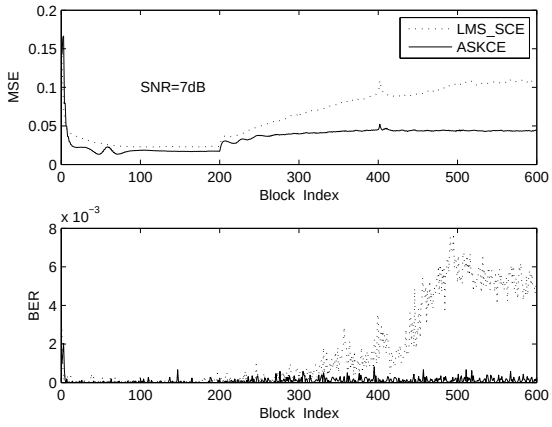

Fig. 5. MSE and BER versus block index at SNR= 7dB.

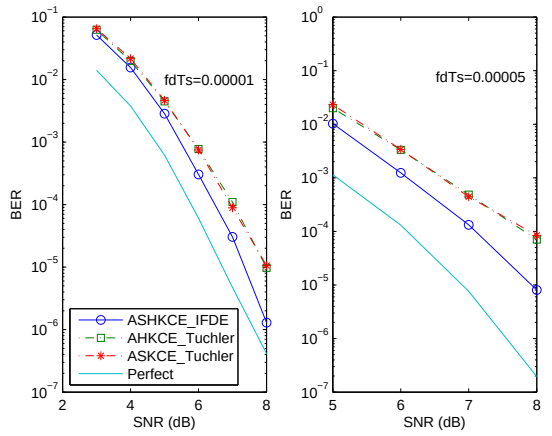

Fig. 6. BER versus SNR at steady state.

frequency domain equalization. Due to the adaptive capabilities of our AFDCE, it is applicable to situations where the channel statistics are unknown or difficult to estimate. Deeper analytical insights into the convergence behavior of AFDCE will be the subject of future work.

REFERENCES

[1] D. Falconer, S. Ariyavisitakul, A. Benyamin-Seeyar, and B. Eidson, "Frequency domain equalization for single-carrier broadband wireless systems," *IEEE Commun. Mag.*, vol. 40, pp. 58–66, Apr. 2002.

[2] C. Douillard, M. Jezequel, C. Berrou, A. Picart, P. Didier, and A. Glavieux, "Iterative correction of intersymbol interference: Turbo equalization," *European Trans. on Telecommunications*, vol. 6, pp. 507–511, Sept.-Oct. 1995.

[3] A. S. R. Koetter and M. Tüchler, "Turbo equalization," *IEEE Signal Processing Mag.*, vol. 21, pp. 67–80, Jan. 2004.

[4] M. Tüchler and J. Hagenauer, "Linear time and frequency domain Turbo equalization," in *Proc. Vehicular Technology Conf., Rhodes, Greece.*, May 2001.

[5] M. Tüchler and J. Hagenauer, "Turbo equalization using frequency domain equalizers," in *Proc. Allerton Conf., Monticello, IL.*, Oct. 2000.

[6] H. Liu, P. Schniter, H. Fu, and R. A. Casas, "A frequency domain Turbo equalization for trellis coded vestigial sideband modulation," in *Proc. IEEE Workshop on Signal Processing Advances in Wireless Communications*, July 2006.

[7] D. Schafhuber, G. Matz, and F. Hlawatsch, "Kalman tracking of time-varying channels in wireless MIMO-OFDM systems," in *Proc. Signals, Systems and Computers Conf., Asilomar, CA. USA.*, Nov. 2003.

[8] D. Schafhuber and G. Matz, "MMSE and adaptive prediction of time-varying channels for OFDM systems," *IEEE Trans. Wireless Communications*, vol. 4, pp. 593–602, Mar. 2005.

[9] R. C. Cannizzaro, P. Banelli, and G. Leus, "Adaptive channel estimation for OFDM systems with Doppler spread," in *Proc. IEEE Workshop on Signal Processing Advances in Wireless Communications*, July 2006.

[10] M. Tüchler, R. Otnes, and A. Schmidbauer, "Performance of soft iterative channel estimation in Turbo equalization," in *Proc. International Communications Conf., New York, USA.*, May 2002.

[11] S. Song, A. C. Singer, and K.-M. Sung, "Soft input channel estimation for Turbo equalization," *IEEE Trans. Signal Processing*, vol. 52, pp. 2885–2894, Oct. 2004.

[12] S. Jiun, J. Coon, R. J. Piechocki, A. Dowler, A. Nix, M. Beach, S. Armour, and J. McGeehan, "A channel estimation algorithm for MIMO-SCFDE," *IEEE Communications Letters*, vol. 8, pp. 555–557, Sept. 2004.

[13] R. Dinis, R. Kalbasi, D. Falconer, and A. Banihashemi, "Channel estimation for MIMO systems employing single-carrier modulations with iterative frequency-domain equalization," in *Proc. Vehicular Technology Conf., Los Angeles, CA. USA.*, Sept. 2004.

[14] W. Liu, L. Yang, and L. Hanzo, "Wideband channel estimation and prediction in single-carrier wireless systems," in *Proc. Vehicular Technology Conf., Stockholm, Sweden.*, May 2005.

[15] C.-J. Park and G.-H. Im, "Efficient cyclic prefix reconstruction for coded OFDM systems," *IEEE Commun. Letter*, vol. 8, pp. 274–276, May 2004.

[16] J. Hagenauer, E. Offer, and L. Papke, "Iterative decoding of binary block and convolutional codes," *IEEE Trans. Information Theory*, vol. 42, pp. 429–445, Mar. 1996.

[17] S. Haykin, *Adaptive Filter Theory*. Prentice-Hall, Upper Saddle River, NJ., 2001.

[18] M. Morelli, L. Sanguinetti, and U. Mengali, "Channel estimation for adaptive frequency-domain equalization," *IEEE Trans. Wireless Communications*, vol. 4, pp. 2508–2518, Sept. 2005.